# Selective venous sampling supports localization of adenoma in primary hyperparathyroidism

Masaya Ikuno[1,2] ⓘ, Takayuki Yamada[3], Yasumoto Shinjo[3],
Tsuyoshi Morimoto[3], Reiko Kumano[3], Kunihiro Yagihashi[3] ⓘ,
Takuyuki Katabami[4] and Yasuo Nakajima[2]

## Abstract

**Background:** Selective venous sampling (SVS) is an invasive localization study for persistent or recurrent hyperparathyroidism.
**Purpose:** To assess the role of SVS in addition to non-invasive imaging for primary hyperparathyroidism (pHPT).
**Material and Methods:** This study was approved by the institutional review board and included 14 patients who underwent SVS and subsequent parathyroidectomy between January 2014 and April 2017 following a clinical diagnosis of pHPT. All patients underwent pre-SVS non-invasive imaging, including ultrasound, computed tomography (CT), and [99mTc]-MIBI scintigraphy, and sensitivity was assessed using the operative and pathological findings.
**Results:** In all but one case, a single parathyroid adenoma was responsible for the pHPT; the remaining case exhibited a chemical response following surgical removal of parathyroid tissue. The sensitivity (%) for ultrasound, CT, [99mTc]-MIBI scintigraphy, and SVS was 76.9, 84.6, 69.2, and 76.9, respectively. SVS yielded positive results in four patients with discordant results and one patient with non-detectable results on imaging. In seven patients, a significant increase in the intact parathyroid hormone level was recognized only in the thyroid veins. The procedure time was in the range of 52–183 min (median = 89.5 min).
**Conclusion:** The addition of SVS to a non-invasive imaging study would be helpful to locate the responsible lesion of pHPT with discordant or non-detectable results on imaging for initial surgical treatment as well.

## Introduction

Primary hyperparathyroidism (pHPT) is a relatively common disease (1–3). Surgery is currently the curative treatment for pHPT, although some patients do not require surgery because they are asymptomatic (4). Currently, minimally invasive parathyroidectomy (MIP) is preferred and appears to cause fewer cases of hypocalcemia and recurrent laryngeal nerve injury as compared with conventional bilateral neck exploration (5–7).

In the era of MIP, surgeons require more precise preoperative localization studies to identify the location of the functioning parathyroid gland and its

[1]Department of Radiology, Sagamihara Kyodo Hospital, Kanagawa, Japan
[2]Department of Radiology, St. Marianna University School of Medicine, Kanagawa, Japan
[3]Department of Radiology, St. Marianna University School of Medicine, Yokohama City Seibu Hospital, Kanagawa, Japan
[4]Division of Metabolism and Endocrinology, Department of Internal Medicine, St. Marianna University School of Medicine, Yokohama City Seibu Hospital, Kanagawa, Japan

**Corresponding author:**
Masaya Ikuno, Sagamihara Kyodo Byoin 2-8-18, Hashimoto Midori-ward, Sagamihara, Kanagawa 252-5188, Japan.
Email: m-ikuno@marianna-u.ac.jp

surrounding structures. These studies usually involve non-invasive imaging examinations such as ultrasound (US) and ^{99m}Tc-Sestamibi (MIBI). Although both methods provide good detectability, some cases remain complicated by non-localizing or discordant results. Selective venous sampling (SVS) is an invasive method of localization (1). The precise localization afforded by SVS should benefit surgeons especially if non-invasive imaging is inconclusive. Several studies have demonstrated the feasibility of SVS (1,8–15); however, to our knowledge, few have evaluated its ability to localize the hyperfunctioning gland in patients indicated for initial surgery.

This study aimed to show the role of SVS in addition to non-invasive imaging for pHPT.

## Material and Methods

### Patients

Institutional review board approval was obtained for this study and the requirement for informed consent was waived due to the retrospective design. Our hospital is a tertiary center with referrals. Twenty-six patients underwent SVS between January 2014 and April 2017 following a clinical diagnosis of pHPT. Twelve asymptomatic patients had been followed up because they were not satisfied with the surgical criteria (16). In total, 13 of 26 patients subsequently underwent parathyroidectomy as initial surgical treatment. Furthermore, one patient previously had undergone a left parathyroidectomy for pHPT; however, the parathyroid adenoma was not identified and the clinical findings did not improve (Tables 1 and 2, Case 3). Consequently, this patient was indicated for repeat surgical treatment for persistent HPT. A total of 14 patients (6 men, 8 women; age range = 17–86 years; median age = 66.5 years) were included in this study.

### Preoperative non-invasive localizing examination

All 14 patients underwent non-invasive localizing examinations, including US, computed tomography (CT), and MIBI scintigraphy, and single photon emission computed tomography (SPECT). For the purposes of this study, we used the findings reported in our institution's radiology reporting system.

### Ultrasound

Each patient underwent an ultrasonographic scan (Aplio ultrasound system; Toshiba Medical System, Kawasaki, Japan) performed by an experienced US technologist using a linear probe with a frequency of 8 MHz. The technologist evaluated suspicious nodules

**Table 1.** Individual patient details illustrating findings, evaluation of imaging results, location of culprit gland, and calcium/iPTH value before and after surgery.

| Case | 1 | 2 | 3 | 4 | 5 | 6 | 7 | 8 | 9 | 10 | 11 | 12 | 13 | 14 |
|---|---|---|---|---|---|---|---|---|---|---|---|---|---|---|
| Age | 66 | 67 | 71 | 79 | 63 | 74 | 64 | 72 | 79 | 17 | 50 | 35 | 86 | 57 |
| Sex | M | F | F | F | M | M | M | F | F | F | F | M | F | M |
| US | × | ○LtL | ○RtL | ○RtL | ○RtU | ○RtL, LtL | ○RtL | × | ○LtL | ○RtL | ○RtL | × | ○Rt | ○Rt |
| CT | ○RtL | ○LtL | ○RtL | ○RtL | ○RtU | ○RtL | ○RtL | × | ○LtL | ○RtL | ○RtL | × | ○Rt | ○Rt |
| MIBI | ○RtL | × | × | ○RtL | × | ○RtL | ○RtL | × | ○LtL | ○RtL | × | ○LtL | ○Rt | ○Rt |
| Site of parathyroidectomy | RtL | LtL | RtU | RtL | RtU | RtL, LtL, LtU | RtL | RtU | LtL | RtL | RtL, RtL, LtL | LtL | RtU | RtU |
| Location | RtL | LtL | RtU | RtL | RtU | RtL | RtL | RtU | LtL | RtL | Unspecified | LtL | RtU | RtU |
| Ca before surgery (mg/dL) | 11.6 | 12 | 10.6 | 10.7 | 11.4 | 11.7 | 11.7 | 14.5 | 12.8 | 9.8 | 9.8 | 11.9 | 11.4 | 10.9 |
| Ca after surgery (mg/dL) | 9.2 | 9.3 | 8.9 | 9.4 | 9.4 | 9 | 9.1 | 9.2 | 9.4 | 9.1 | 9.1 | 10.2 | 9.4 | 9.2 |
| iPTH before surgery (pg/mL) | 93 | 80 | 80 | 189 | 127 | 91 | 260 | 332 | 78 | 442 | 97 | 128 | 581 | 144 |
| iPTH after surgery (pg/mL) | 16 | 42 | None | 30 | 51 | 10 | 47 | 55 | 33 | 56 | 63 | 46 | 63 | 21 |

○, location was suggested; ×, non-detectable (or undetected); RtL, right lower; RtU, right upper; LtL, left lower; LtU, left upper; Rt, right side; Ca, serum calcium.

**Table 2.** Results of iPTH value (pg/mL) at each sampling point, predictive site on SVS, location of culprit gland, and procedure time.

| Case | 1 | 2 | 3 | 4 | 5 | 6 | 7 | 8 | 9 | 10 | 11 | 12 | 13 | 14 |
|---|---|---|---|---|---|---|---|---|---|---|---|---|---|---|
| 1. Rt. jugular (distal site of STV) | 115 | 128 | 87 | 131 | 115 | 108 | 221 | 138 | 121 | 1100 | 56 | 117 | 591 | 138 |
| 2. Rt. jugular (joining site of STV) | 104 | 123 | 97 | 137 | 1550* | 106 | 274 | 133 | 110 | 9800* | 63 | 118 | 695 | 128 |
| 3. Rt. jugular (proximal site of STV) | 103 | 124 | 82 | 143 | 371* | 121 | 238 | 150 | 123 | 3340* | 87 | 120 | 1070 | 125 |
| 4. Rt. jugular (joining site of MTV) | 412* | 106 | 88 | 140 | 423* | 203 | 233 | 158 | 144 | 3040* | 60 | 121 | 676 | 131 |
| 5. Rt. jugular (proximal site of MTV) | 431* | 121 | 1910* | 142 | 803* | 231* | 215 | 142 | 136 | 2690* | 60 | 110 | 649 | 153 |
| 6. Rt. brachiocephalic | 146 | 112 | 173 | 129 | 235* | 177 | 268 | 151 | 159 | 2210* | 61 | 111 | 660 | 237 |
| 7. Rt. ITV | 69 | 14,200* | 94 | Impossible | NA | 484* | 15,200* | 6960* | Impossible | 1150* | Impossible | 151 | 4370* | 2170* |
| 8. d Lt. ITV (distal) | 94 | 2950* | 85 | Impossible | NA | NA | 294 | 166 | Impossible | 1450* | 1880* | 3270* | 3620* | 129 |
| 8. p Lt. ITV (proximal) | | | | | | | | | | | | | | |
| 9. Lt. jugular (distal site of STV) | 104 | 127 | 94 | 126 | 107 | 105 | 233 | 146 | 121 | 623 | 63 | 130 | 554 | 125 |
| 10. Lt. jugular (joining site of STV) | 102 | 140 | 98 | 135 | 122 | 121 | 229 | 171 | 124 | 573 | 98 | 108 | 584 | 138 |
| 11. Lt. jugular (proximal site of STV) | 107 | 156 | 94 | 138 | 123 | 142 | 241 | 163 | 119 | 617 | 70 | 120 | 630 | 147 |
| 12. Lt. jugular (joining site of MTV) | 102 | 126 | 83 | 137 | 119 | 118 | 237 | 146 | 134 | 630 | 74 | 121 | 641 | 140 |
| 13. Lt. jugular (proximal site of MTV) | 100 | 153 | 87 | 116 | 115 | 111 | 220 | 141 | 124 | 641 | 74 | 121 | 640 | 138 |
| 14. Lt. brachiocephalic | 100 | 130 | 88 | 158 | 111 | 99 | 232 | 149 | 175 | 620 | 68 | 115 | 644 | 145 |
| 15. SVC | 107 | 156 | 87 | 101 | 102 | 108 | 230 | 230 | 112 | 1110 | 84 | 173 | 898 | 112 |
| 16. Rt. STV | | | | | 16,100* | 131 | 301 | NS | NS | 1100 | 2420* | 99 | 2710* | 7630* |
| 17. Rt. MTV | | | | | 6020* | Impossible | NA | NA | Impossible | 2600* | 3850* | Impossible | NA | 8610* |
| 18. Lt. STV | | | | | NS | 107 | 236 | NS | NS | 834 | 971* | 217 | 661 | 151 |
| 19. Lt. MTV | | | | | NS | 210 | NA | NA | Impossible | 640 | NA | 181 | NA | Impossible |
| Predictive site | ◯RtL | ◯LtL | ◯RtU | × | ◯RtU | ◯RtL | ◯RtL | ◯RtL | × | △Rt | ×RtU, Lt | ◯LtL | ×Rt, LtL | △Rt |
| Location | RtL | LtL | RtU | RtL | RtU | RtL | RtL | RtL | LtL | RtL | unspecified | LtL | RtU | RtU |
| Procedure time (min) | 83 | 183 | 80 | 113 | 81 | 139 | 77 | 86 | 52 | 92 | 87 | 124 | 108 | 149 |

*Significant value of iPTH.

Rt, right; Lt, left; STV, superior thyroid vein; MTV, middle thyroid vein; ITV, inferior thyroid vein; SVC, superior vena cava; NS, not selected; NA, not applicable; ◯, probable; △, possible; ×, non-detectable; RtL, right lower; RtU, right upper; LtL, left lower; Impossible, the branch could not be catheterized.

at and/or adjacent to the thyroid gland and recorded the findings in the radiological reporting system.

## MIBI scintigraphy and SPECT

Dual-phase scintigraphy was performed 20 min following radiotracer administration (600–740 MBq of MIBI) and at 2 h post injection. Planar and SPECT images were obtained using a two-head scanner (Symbia Evo Excel, e.cam; Siemens Medical Solutions, Malvern, PA, USA). A nodule exhibiting retained uptake in the delayed phase was considered a suspicious lesion.

## CT scanning technique and image analysis

All contrast-enhanced CT images from the skull base to the lower edge of the aortic arch were obtained on a multidetector-row CT scanner (Aquilion 64; Toshiba Medical Systems, Kawasaki, Japan). Iodinated contrast material (300 mg I/mL) at a dosage of 2 mL/kg was injected at a rate of 1.5 mL/s. At 90 s post injection, the CT images were obtained using the following parameters: collimation $= 32 \times 0.5$ mm; tube voltage $= 120$ kVp; tube current $= 200$ mA; gantry rotation time $= 0.75$ s; and beam pitch $= 0.844$ (helical pitch $= 27$). The scan data were reconstructed to axial images with slice thicknesses of 1 mm and coronal images with slice thicknesses of 2–3 mm without section interval overlaps. The imaging field of view was $240 \times 240$ mm and the pixel size was $0.468 \times 0.468$ mm.

The radiologists performing the SVS evaluated the suspicious nodule before venous sampling with US and MIBI examination data. Thyroid vein anatomy was recorded on CT scans in the manner described in a previous report on preparatory practices for SVS (17). First, the superior and middle thyroid veins and the sites at which these veins joined the internal jugular veins were identified. Second, the inferior veins and the sites at which they joined the brachiocephalic veins were identified using transverse and coronal images in accordance with a previous study reporting the various branching patterns of inferior veins (18).

## Selective venous sampling

After puncturing the right femoral vein, a 4-Fr multi-purpose, Berenstein catheter (Heartcath, 100 cm or 120 cm; Terumo, Tokyo, Japan) or 4.2-Fr H1H catheter (IR catheter, 100 cm; Hanako, Saitama, Japan) was used to obtain blood samples at the bilateral jugular and brachiocephalic veins. The initial sampling points at the jugular vein were set by the initial protocol until December 2014; however, beginning in January 2015, these sites were modified by the joining sites of the thyroid veins as determined by CT scans. Of the thyroid veins, only the left inferior thyroid vein was sampled until December 2014 (Fig. 1a). Subsequently, attempts were made to catheterize all thyroid veins (Fig. 1b).

When the left interior thyroid vein was catheterized, retrograde venogram was performed to opacify the
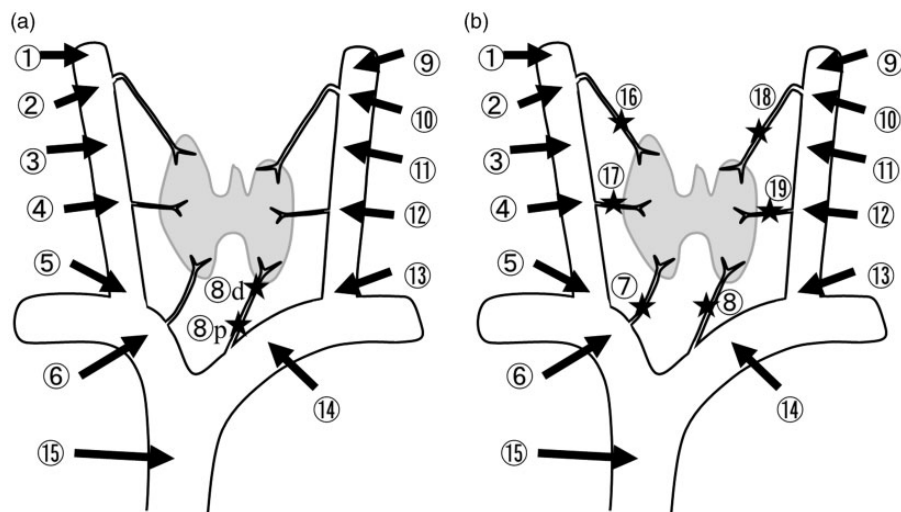


**Fig. 1.** Sampling points for selective venous sampling (SVS). (a) Initial protocol sampling points until December 2014. Only the left inferior thyroid vein was sampled at the distal and proximal sites. (b) Sampling points of the modified protocol since January 2015. An attempt was made to catheterize every thyroid vein. 1, 9, the upper superior thyroid vein; 2, 10, the joining site of the superior thyroid vein; 3, 11, between the superior and middle thyroid veins; 4, 12, the joining site of the middle thyroid vein; 5, 13, the joining site of the internal jugular and subclavian veins; 6, the right brachiocephalic vein; 7, the right inferior thyroid vein; 8, the left inferior thyroid vein; 14, the left brachiocephalic vein; 15, the superior vena cava; 16, the right superior thyroid vein; 17, the right middle thyroid vein; 18, the left superior thyroid vein; 19, the left middle thyroid vein.

**Fig. 2.** A 67-year-old female patient with primary hyperparathyroidism (Case 11). A retrograde venogram from the common trunk of the inferior thyroid veins (7 and 8) shows the superior (16 and 18) and right middle (17) thyroid veins through the venous network.



**Fig. 3.** A 64-year-old male patient with primary hyperparathyroidism (Case 7). A retrograde venogram from the left superior thyroid vein is shown. The bilateral middle thyroid veins are not identified. Other thyroid veins are opacified through the venous network. A significant increase in the intact PTH was recognized only in the right inferior thyroid vein (7), and the SVS localization diagnosis was the right lower quadrant, which was considered probable.

other thyroid veins through their connections (Figs. 2 and 3), which enabled us to determine the sampling point in the catheterized thyroid vein and confirm the existence of a particular thyroid vein that was not depicted on CT scans. Next, a 2.3-Fr microcatheter with a side hole (Gold Crest; HI-LEX Co., Hyogo, Japan) was used in a coaxial manner. We introduced the microcatheter into both the right and left thyroid veins where they formed a common trunk and collected more blood samples from these veins when possible. The samples were not collected if we could not visualize a certain thyroid vein on CT scan or retrograde venogram. The intact PTH (iPTH) level was measured in all blood samples and the SVS procedure time was recorded from the medical charts.

## Interpretation of the SVS results

We defined a significant increase in iPTH concentration as a twofold increase relative to the level in the superior vena cava. The responsible lesion sites were divided into four quadrants (right upper, right lower, left upper, and left lower) assuming there were four parathyroid glands. The result was defined as probable if the responsible quadrant could be clearly specified, as possible if we could not localize the quadrant but could localize the approximate region (e.g. left or right side), and as non-detectable if we could not localize the approximate region or failed to observe a significant increase in iPTH. Probable and possible were both considered positive results.
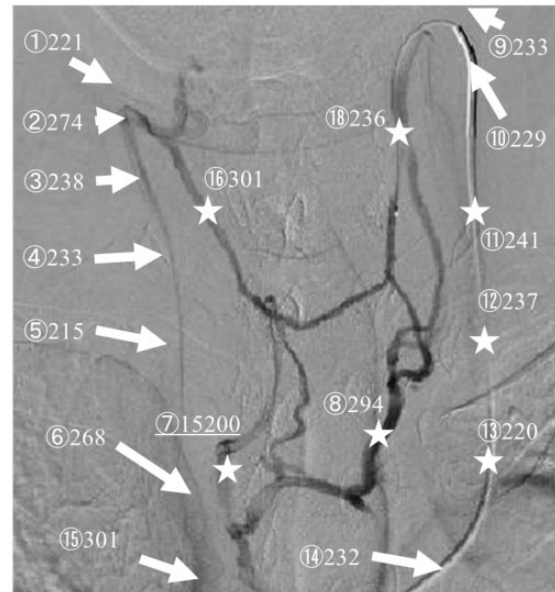
## Correlations with operative findings and postoperative biochemical responses

The suspicious lesions predicted by US, CT, and MIBI were compared with the sites of responsible parathyroid lesions according to the operative and pathological findings; the SVS results were also correlated with the operative and pathological findings. Sensitivity was calculated for non-invasive studies and SVS, respectively.

The post-parathyroidectomy iPTH values were obtained from the patients' medical charts. Treatment was considered successful if the iPTH value improved to within the normal range.

## Results

### Operative findings and postoperative biochemical responses

Table 1 shows the results of non-invasive imaging studies, the operative locations of the responsible glands, and the biochemical responses. Pathologically, a single parathyroid adenoma was the responsible lesion in all but one case. In one patient (Case 11), surgical treatment was performed for three parathyroid glands; however, an adenoma was not detected pathologically, thus the responsible lesion was unspecified. Therefore,

13 patients in whom the responsible lesion was specified were the subjects of the sensitivity calculation.

The serum calcium and iPTH values decreased postoperatively in all 14 patients, including Case 11 (Table 1). Accordingly, all treatments were considered successful in terms of the biochemical response.

### Noninvasive localization studies

Of the 13 adenomas (13 patients), US depicted ten, CT scans depicted 11, and MIBI scintigraphy depicted nine; the sensitivity of US, CT, and MIBI scintigraphy was 76.9%, 84.6%, and 69.2%, respectively. The cross-sectional imaging and MIBI scintigraphy findings were consistent in eight patients in whom the responsible adenoma quadrants were consistent with those identified in imaging studies. However, the two types of studies yielded discordant results in four of the 13 patients; in the remaining patient, none of the non-invasive imaging studies were able to depict the suspicious lesion.

### Selective venous sampling

Table 2 presents the iPTH values at all SVS points. No patients developed complications related to SVS. The procedure time was 52–183 min (median = 89.5 min).

SVS detected the quadrant suspected of being responsible for the culprit gland in eight of 13 patients and the responsible side in two of 13 patients. In the other three patients, the thyroid veins could not be sampled and no significant increase in iPTH was observed in two patients, and it could not be even localized approximate region in one patient; accordingly, these cases were defined as non-detectable. The sensitivity of SVS was 76.9%.

Notably, in the patients with a single adenoma, SVS yielded positive results in four patients with discordant results and one patient with non-detectable results on non-invasive imaging studies (probable in all patients). Conversely, three patients in whom SVS was non-diagnostic had concordant findings on non-invasive localization.

Significant increases in iPTH levels were identified in the jugular veins of five of 14 patients and the greatest iPTH gradient was noted in the thyroid veins in two patients (Fig. 4). In seven patients, a significant increase was recognized only in the thyroid veins and four of these patients had a steep increase in iPTH concentration in the inferior thyroid vein; however, it did not increase in the brachiocephalic vein near the joining site.

## Discussion

There are two important clinical findings regarding SVS. First, SVS is feasible in patients with discordant or non-detectable non-invasive imaging study results. Second, SVS of blood from the thyroid veins was beneficial.

Although diagnostic non-invasive imaging studies are able to localize lesions (2,19–24), discordant or equivocal results are often obtained from multiple examinations. Our study revealed that SVS yielded positive (i.e. probable or possible) results in all patients with discordant or non-detectable findings and has been reported to yield a high sensitivity (1,11–15). Two previous studies found that SVS enabled localization of responsible lesions in affected patients with non-localizing or discordant findings (25,26). Therefore, the performance of SVS in addition to non-invasive imaging studies could have a role in improving the confidence of predictions as well as the accuracy of localization diagnoses.

We found that it was beneficial to collect samples selectively from the thyroid vein whenever possible; however, few studies have discussed the importance of the sampling point in diagnostic ability. In the present study, we observed the greatest iPTH gradient in the thyroid veins, although two patients also exhibited elevated iPTH levels in the jugular veins. In addition, seven patients had significant increases in iPTH levels only in the thyroid veins. Additionally, the iPTH level decreased rapidly as the sampling point became incrementally distant from the lesion area. Gimm et al. suggested that SVS of the thyroid veins would provide detailed spatial resolution (1); therefore, if the thyroid veins are sampled selectively to the extent possible, we can expect a higher sensitivity. Conversely, catheterization of multiple thyroid veins is time consuming and can be technically challenging. SVS complexity seems to increase in accordance with the variability in the structure of the thyroid veins. The bilateral superior, middle, and inferior thyroid veins have been depicted in the literature as typical scenarios (8,9); however, multidetector-row CT scans have revealed variations in the structure of the thyroid veins (18). Several patterns of inferior veins featuring different numbers and joining sites to the brachiocephalic vein have been observed and the middle veins are frequently absent. Therefore, familiarity with the thyroid vein anatomy should improve the success of thyroid vein catheterization (17). Retrograde venous angiography can depict the venous network in the thyroid region and can thus assist clinicians in determining sampling points in the thyroid veins.

This study had several limitations. First, the blood sampling method changed during the study period, i.e. the procedure was not consistent. Second, we could not selectively obtain samples from every thyroid vein in all cases. Third, all pathologically proven responsible lesions in 13 patients were identified as single
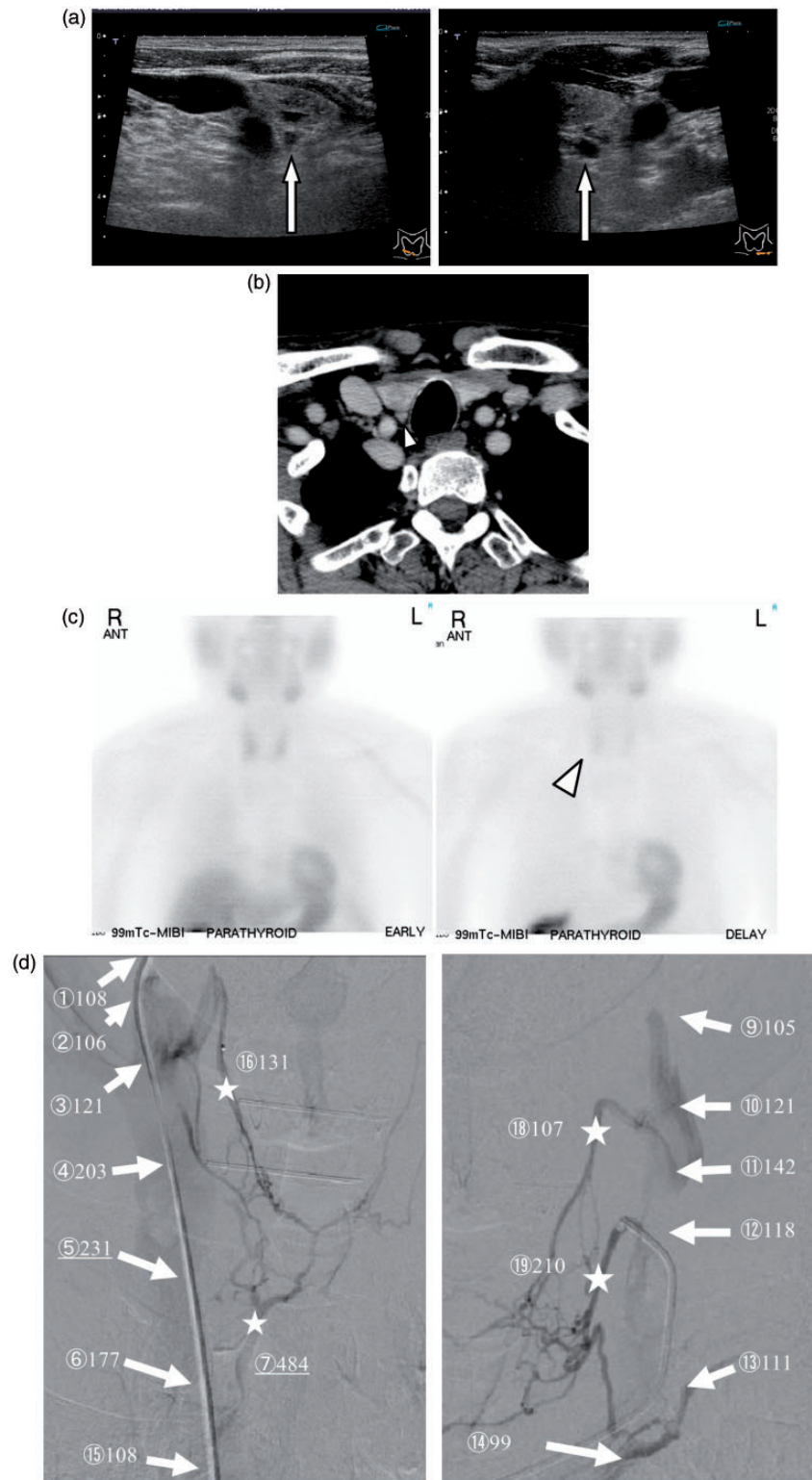
**Fig. 4.** A 74-year-old male patient with primary hyperparathyroidism (Case 6) who was pathologically diagnosed with parathyroid adenoma in the right lower gland. (a) US showed the low echoic nodule caudal to both thyroid lobes, which could not be distinguished from the lymph nodes. (b) CT demonstrated a small nodule caudal to the right thyroid lobe. (c) MIBI in the delayed phase showed slightly increased uptake in the right thyroid lobe (arrowhead), which was ambiguous as a significant feature. (d) A retrograde venogram from the right superior thyroid vein and left middle thyroid vein are shown, and the values of intact PTH (iPTH) were noted at the veins. The most significant increase in iPTH was recognized in the right inferior thyroid vein (7) and a significant increase in iPTH was also revealed in the right jugular vein where it joins with the middle thyroid vein (5). The SVS localization diagnosis was probably the right lower quadrant.

adenomas. In the remaining patient, multiple quadrants were identified on SVS as suspicious, and even though the resected tissue included parathyroid tissue, an adenoma was not pathologically confirmed. Although the patient experienced symptom relief and exhibited a biochemical response, the feasibility of SVS for multinodular lesions remains unclear. Fourth, recent reports have described improved sensitivity rates for four-dimensional CT and SPECT/CT (27–30); however, these modalities were not used in the present study, and their inclusion might have altered the significance of SVS.

In conclusion, the use of SVS in addition to non-invasive imaging studies could have a role in improving confidence regarding the localization of a responsible lesion. We considered it beneficial to collect samples selectively from the thyroid veins whenever possible after anatomical imaging to determine the site that would yield the greatest iPTH gradient and thus the best SVS spatial resolution.

## Declaration of conflicting interests

## Funding

## ORCID iDs

Masaya Ikuno   http://orcid.org/0000-0002-8574-8557
Kunihiro Yagihashi   http://orcid.org/0000-0002-3223-0842

## References

1. Gimm O, Arnesson LG, Olofsson P, et al. Super-selective venous sampling in conjunction with quickPTH for patients with persistent primary hyperparathyroidism: report of five cases. Surg Today 2012;42:570–576.
2. Loevner LA. Imaging of the parathyroid glands. Semin Ultrasound CT MR 1996;17:563–575.
3. Johnson NA, Carty SE, Tublin ME. Parathyroid imaging. Radiol Clin North Am 2011;49:489–509.
4. Brasso K, Karstrup S, Lundby CM, et al. Surgical treatment of primary hyperparathyroidism. Dan Med Bull 1994;41:585–588.
5. Noureldine SI, Gooi Z, Tufano RP. Minimally invasive parathyroid surgery. Gland Surg 2015;4:410–419.
6. Singh Ospina NM, Rodriguez-Gutierrez R, Maraka S, et al. Outcomes of parathyroidectomy in patients with primary hyperparathyroidism: a systematic review and meta-analysis. World J Surg 2016;40:2359–2377.
7. Smit PC, Borel Rinkes IH, van Dalen A, et al. Direct, minimally invasive adenomectomy for primary hyperparathyroidism: An alternative to conventional neck exploration? Ann Surg 2000;231:559–565.
8. Shimkin PM, Powell D, Doppman JL, et al. Parathyroid venous sampling. Radiology 1972;104:571–574.
9. Ogilvie CM, Brown PL, Matson M, et al. Selective parathyroid venous sampling in patients with complicated hyperparathyroidism. Eur J Endocrinol 2006;155:813–821.
10. Reidel MA, Schilling T, Graf S, et al. Localization of hyperfunctioning parathyroid glands by selective venous sampling in reoperation for primary or secondary hyperparathyroidism. Surgery 2006;140:907–913; discussion 913.
11. Chaffanjon PC, Voirin D, Vasdev A, et al. Selective venous sampling in recurrent and persistent hyperparathyroidism: indication, technique, and results. World J Surg 2004;28:958–961.
12. Lumachi F, Ermani M, Basso S, et al. Localization of parathyroid tumours in the minimally invasive era: which technique should be chosen? Population-based analysis of 253 patients undergoing parathyroidectomy and factors affecting parathyroid gland detection. Endocr Relat Cancer 2001;8:63–69.
13. Eloy JA, Mitty H, Genden EM. Preoperative selective venous sampling for nonlocalizing parathyroid adenomas. Thyroid 2006;16:787–790.
14. Witteveen JE, Kievit J, van Erkel AR, et al. The role of selective venous sampling in the management of persistent hyperparathyroidism revisited. Eur J Endocrinol 2010;163:945–952.
15. Sugg SL, Fraker DL, Alexander R, et al. Prospective evaluation of selective venous sampling for parathyroid hormone concentration in patients undergoing reoperations for primary hyperparathyroidism. Surgery 1993;114:1004–1009. discussion 1009–1010.
16. Bilezikian JP, Brandi ML, Eastell R, et al. Guidelines for the management of asymptomatic primary hyperparathyroidism: summary statement from the Fourth International Workshop. J Clin Endocrinol Metab 2014;99:3561–3569.
17. Yamada T, Ikuno M, Shinjo Y, et al. Selective venous sampling for primary hyperparathyroidism: how to perform an examination and interpret the results with reference to thyroid vein anatomy. Jpn J Radiol 2017;35:409–416.
18. Tomita H, Yamada T, Murakami K, et al. Anatomical variation of thyroid veins on contrast-enhanced multidetector row computed tomography. Eur J Radiol 2015;84:872–876.
19. Cheung K, Wang TS, Farrokhyar F, et al. A meta-analysis of preoperative localization techniques for patients with primary hyperparathyroidism. Ann Surg Oncol 2012;19:577–583.
20. Gotthardt M, Lohmann B, Behr TM, et al. Clinical value of parathyroid scintigraphy with technetium-99m methoxyisobutylisonitrile: discrepancies in clinical data and a systematic metaanalysis of the literature. World J Surg 2004;28:100–107.

21. Erbil Y, Barbaros U, Yanik BT, et al. Impact of gland morphology and concomitant thyroid nodules on pre-operative localization of parathyroid adenomas. Laryngoscope 2006;116:580–585.

22. Sukan A, Reyhan M, Aydin M, et al. Preoperative evaluation of hyperparathyroidism: the role of dual-phase parathyroid scintigraphy and ultrasound imaging. Ann Nucl Med 2008;22:123–131.

23. Zald PB, Hamilton BE, Larsen ML, et al. The role of computed tomography for localization of parathyroid adenomas. Laryngoscope 2008;118:1405–1410.

24. Berber E, Parikh RT, Ballem N, et al. Factors contributing to negative parathyroid localization: an analysis of 1000 patients. Surgery 2008;144:74–79.

25. Sun PY, Thompson SM, Andrews JC, et al. Selective parathyroid hormone venous sampling in patients with persistent or recurrent primary hyperparathyroidism and negative, equivocal or discordant noninvasive imaging. World J Surg 2016;40:2956–2963.

26. Jones JJ, Brunaud L, Dowd CF, et al. Accuracy of selective venous sampling for intact parathyroid hormone in difficult patients with recurrent or persistent hyperparathyroidism. Surgery 2002;132:944–950. discussion 950–951.

27. Hoang JK, Sung WK, Bahl M, et al. How to perform parathyroid 4D CT: tips and traps for technique and interpretation. Radiology 2014;270:15–24.

28. Lavely WC, Goetze S, Friedman KP, et al. Comparison of SPECT/CT, SPECT, and planar imaging with single- and dual-phase (99m)Tc-sestamibi parathyroid scintigraphy. J Nucl Med 2007;48:1084–1089.

29. Day KM, Elsayed M, Beland MD, et al. The utility of 4-dimensional computed tomography for preoperative localization of primary hyperparathyroidism in patients not localized by sestamibi or ultrasonography. Surgery 2015;157:534–539.

30. Kelly HR, Hamberg LM, Hunter GJ. 4D-CT for preoperative localization of abnormal parathyroid glands in patients with hyperparathyroidism: accuracy and ability to stratify patients by unilateral versus bilateral disease in surgery-naive and re-exploration patients. AJNR Am J Neuroradiol 2014;35:176–181.